This is to certify that the

thesis entitled

AN APPLICATION OF FINITE ELEMENTS METHOD TO REDUCE NOISE INSIDE A CAR CAVITY

presented by

Carlos Eduardo Lopes

has been accepted towards fulfillment
of the requirements for

_______ degree in _______

MASTER OF SCIENCE
Department of Mechanical Engineering

Major professor
Alejandro Diaz

Date May 22, 1998

AN APPLICATION OF FINITE ELEMENTS METHOD TO REDUCE NOISE INSIDE A CAR CAVITY

By

Carlos Eduardo Lopes

A THESIS

Submitted to
Michigan State University
in partial fulfillment of the requirements
for the degree of

MASTER OF SCIENCE

Department of Mechanical Engineering

1998

ABSTRACT

AN APPLICATION OF FINITE ELEMENT METHOD TO REDUCE NOISE INSIDE A CAR CAVITY

By

Carlos Eduardo Lopes

Dynamic frequency response is used for different applications in noise vibration and harshness analysis of mechanical and structural systems subject to external loads generated by oscillation in some form of periodic motion. This interaction can be noticed in an automobile compartment, where the interior sound pressure can result from input forces from the road and from the power train exciting the vehicle compartment panels. In this study an accurate characterization of this enclosed medium is presented using a finite element model for an absorbent porous material and its interface with adjacent acoustical media. The finite element system is based on a theory presented in terms of static resistivity and the effective density of the porous medium. The model is specifically developed to analyze the effects of the shape of foam lining on the reduction of sound pressure level, inside a vehicle interior. Results show that for a lining of foam that occupies a restricted volume in an acoustic cavity, the reduction of the level of sound pressure is related more with the shape of the foam than with the amount of foam implemented. Better results for the sound pressure level were found for shapes of lining with 30% to 40 % less foam material applied, as compared to the same restricted volume full of foam.

To my parents for their strong will and guidance,

To my brother for the example you have provided me and

To my son for the main reason of this endeavor.

ACKNOWLEDGEMENTS

I would like to express my sincere gratitude to Iochpe Maxion Foundation and also to Iochpe-Maxion S.A. for sponsoring me in the pursuit of this academic program.

My special appreciation goes to my major professor, Dr Alejandro Díaz for his academic guidance and advise, encouragement and friendship.

Thanks also to my friends in the Engineering Department and especially to Joe DeRose, our shared interests and open discussions have formed the basis for a lasting friendship.

TABLE OF CONTENTS

LIST OF TABLES

LIST OF FIGURES

NOMENCLATURE

c	Speed of Sound [m/s]
p	Acoustic Pressure [N/m^2]
ρ	Density [Kg/ m^3]
ρ_0	Static Density [Kg/ m^3]
w	Frequency [Hz]
w_n	Natural Frequency [Hz]
α, β	Rayleigh Damping Coeficients
[C]	Damping Matrix
K	Structure Factor
L	Length of the tube [m]
N	Shape Functions for 4 Node Rectangular Element
[P]	Kinetic Energy Matrix
Q	Prescribed Volume Velocity [m/s]
R	Resistivity [Rayls/m]
[S]	Strain Energy Matrix
U	Acoustical Particle Velocity [m/s]
Ω	Porosity

CHAPTER 1

INTRODUCTION

Excessive noise and vibration are among the major problems facing today's vehicle designers, and much work has being carried out aimed at improving the understanding of the relation among noise, source characteristics and insulation. Noise inside a vehicle is primarily caused by the vibrating surfaces enclosing the passenger compartment. Since this is a confined space, its air resonances (normally referred to as cavity resonances) have considerable influences in the noise generation process.

Although elastic porous materials such as foams are widely used in automobile interior noise control, complete numerical models of these materials have only recently become available. As a result, it is only now becoming possible to design optimal foam treatments numerically.

Early work related to the finite element analysis of sound absorbing materials was performed for fibrous or rigid porous materials such as glass fiber or open cell foam. Craggs [1] derived an absorption finite element for an extended reaction limp porous material and showed that finite size, extended reaction linings behave differently than do locally reacting liners owing to the transverse propagating modes in a duct. Craggs [2] subsequently used that element to study both wave propagation in ducts and the response of small enclosures lined with bulk reacting materials. A much earlier paper by Scott [3] also showed that at least for sound transmission in ducts the liner is best considered as having a bulk reaction. Later, Astley and Cummings [4] calculated the modal attenuation in a uniform flow duct lined in all four side walls with bulk reacting porous materials by using a finite element analysis, and compared the predicted modal axial attenuation rate, phase speed and transverse pressure profile with measured data. More recently, Munjal [5] proposed a finite element model for predicting the reflection characteristics of a fibrous wedge in an impedance tube. His prediction was compared with the experimental results and the effects of the wedge dimensions and flow resistivity on the reflection coefficient were illustrated. In all these previous works, governing differential equations for porous materials were used that were derived from a generalized Rayleigh model in which the porous material's fibers were assumed to have either zero (limp) or infinite (rigid) stiffness. In either case, only one longitudinal wave is allowed to propagate within the porous material.

Elastic porous materials such as foams generally differ from limp or rigid glass fiber and other fibrous materials in the number of wave types that can propagate within them, as discussed by Bolton [6]. Zwikker and Kosten [7] noted that an elastic porous material such as partially reticulated foam can convey two longitudinal wave types, while only a single longitudinal wave is significant in fibrous media that can be modeled as either limp or rigid. Analytical wave propagation theories have been developed that can account for all wave types that propagate within elastic porous materials such as polyurethane foams as described by Bolton [6]. Those theories can be used to model planar foam treatments (laterally infinite homogeneous foam layers, for example) owing to the classical plane wave solution techniques. Based on these theories, in this study a foam finite element model that can be coupled with acoustic finite elements has been developed. The behavior of the foam is governed by bulk properties such as resistivity and porosity and the results of the coupling procedure were verified through a comparison with analytical and experimental results. The basis for constructing the finite element model is a variational principle given by Morse and Ingard [8], and the formulation is based on a generalized Rayleigh model of the absorbing material in which isotropic properties and rigid fibers are assumed. The output of the finite element is pressure for a two dimensional model having rigid boundaries. In order to evaluate the effect of the shape of foam and respective sound pressure level reduction, different distribution of foam layers were assumed.

In what follows the equations are those derived from a generalized Rayleigh model of the material as given by Morse and Ingard [8]. It is assumed that the resistivity is constant and the effect of the material on the entrapped air is considered by introducing the porosity of the foam.

CHAPTER 2

MODELING ACOUSTIC PRESSURE RESPONSE

2.1 Acoustic Cavity Theory

A typical acoustic enclosure is sketched in Figure 1, a domain Ω^a filled with a medium (fluid) that transmits a linear acoustic wave. If the volume of air contained in this enclosure is excited by a velocity U over the surface S_1 and all the remaining boundaries are hard, the equations of conservation of mass and adiabatic gas law for this problem are, respectively,

$$\rho_0 \nabla . U = -\frac{\partial \rho}{\partial t} \qquad on \;\; \Omega^a \qquad (1)$$

and

$$\frac{\partial \rho}{\partial t} = \frac{1}{c^2}\frac{\partial p}{\partial t}$$

where $\nabla . U \equiv div(U)$

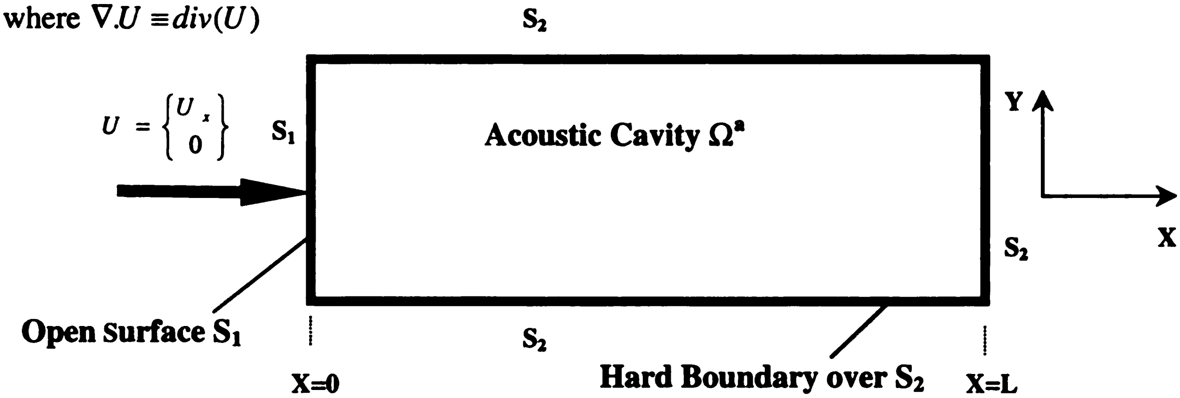

Figure 1 A rectangular acoustic enclosure with a velocity distribution over the surface S1 and a hard boundary over S2.

If a harmonic form e ^{jwt} for ρ is assumed then the fluctuating component of density $\partial\rho/\partial t$ can be eliminated, leading to the equation

$$\nabla . U = \frac{-jw}{\rho_0 c^2} p \tag{2}$$

where U is the particle velocity, p is the acoustic pressure, ρ_0 is the ambient equilibrium density and c is the speed of sound. The application of Newton's second law to the element mass leads to the equation

$$-\nabla p = \rho U = j w \rho_0 U \tag{3}$$

If the velocity U is eliminated between equations (2) and (3), the result is the Helmholtz equation for the domain Ω^a

$$\nabla^2 p - \left(\frac{w}{c}\right)^2 p = 0 \tag{4}$$

The boundary conditions are

1- A uniform velocity applied at the open end

$$\frac{\partial p}{\partial x} = U \ e^{jwt} \quad for\ (x, y) \in S_1$$

2- A normal velocity U.n = 0 at the hard wall

$$\nabla p . n = 0 \qquad for\ (x, y)\ \in S_2$$

where n is the outward normal to the boundary

2.2 Formulation of an Acoustic Finite Element

An acoustic finite element is derived from a variational principle whose stationary values lead to the wave equation and the conditions prevailing at the boundary. A suitable functional F, whose first variation leads to the Helmholtz equation (4), is shown (eq. (5))

$$F = \frac{1}{2}\int_{\Omega^e} \left[(\nabla p . \nabla p) - \left(\frac{w}{c}\right)^2 p^2 \right] \; dA \qquad (5)$$

where w is frequency, c is the speed of sound and p is pressure. Equation (5) is used as the basis of a finite element formulation [3]. Within the domain the pressure is discretized using:

$$p(x, y) = \sum_{i=1}^{4} p_{ei} \, N_{ei} \, (x, y)$$

where each N_{ei} (x,y) is a (bilinear) shape function associated with the *i*-th degree of freedom of element *e*, a four node quadrilateral and p_{ei} is the nodal pressure.

Substituting this approximation into the functional yields

$$F = \sum_e \frac{1}{2} p_e{}^T [S_e - P_e] p_e \qquad (6)$$

where the sum is understood in the sense of assembly,

$$(S_e)_{ij} = \int_e \left(\frac{\partial N_i}{\partial x}\frac{\partial N_j}{\partial x} + \frac{\partial N_i}{\partial y}\frac{\partial N_j}{\partial y} \right) dA$$

and

$$(P_e)_{ij} = \left(\frac{w}{c}\right)^2 \int_e (N_i \; N_j) dA$$

The stationary values of F in equation (6), give the finite element equations for the undamped problem

$$([S]-[P])\{p\}=0 \tag{7}$$

where [P] is the kinetic energy matrix and [S] is the strain energy matrix resulting from the assembly of the element matrices P_e and S_e, respectively.

2.3 Energy Dissipation

Damping causes energy losses in the system and also phase differences in the pressure at various locations. The complete description of the pressure then requires information on the phase angle as well as the amplitude. The usual way to approach this problem is by means of a complex notation for p, as discussed by Craggs [9]. Thus the discretized form of the damped wave equation is

$$(-[P]+j\rho w[C]+[S])p=0 \tag{8}$$

with boundary conditions

$$\begin{aligned} -\nabla p.n &= jw\rho\, U \quad && at\ x=0 \\ \nabla p.n &= 0 && at\ x=S_2 \end{aligned}$$

The damping matrix [C] for the acoustic cavity was assumed to be of the form [C]=α[P]+β[S] (i.e., Rayleigh damping), where α and β are known coefficients that will be adjusted experimentally.

2.4 Results for the Acoustic Finite Element Model

In order to verify the finite element model we compared its output with analytical results. The dimensions of the model were defined based on a variation of the experiment conducted by A. J. Hull [10], which will be described in detail in Section 3.4. One of the main reasons for choosing the geometry of this experiment is because A. J. Hull performed his experiment with a layer of foam at the end of the tube, measuring the response of the cavity with foam and plotting the results. These results will be used in section 3.5 to validate the approach for the assembly air-foam in the finite element model (clearly, the geometry in the experiment is axisymmetric while the finite element is not. Nevertheless, results from the experiment can be used to calibrate the finite element model). In addition, the dimensions of the experiment can be compared with one segment from the floor up to the roof of a vehicle interior and the results from this present study can be extended to characterize the noise and its reduction inside the vehicle. Lastly, the experiment is still available at the Laboratory of Acoustics and can be setup in the future to validate all the results from this study

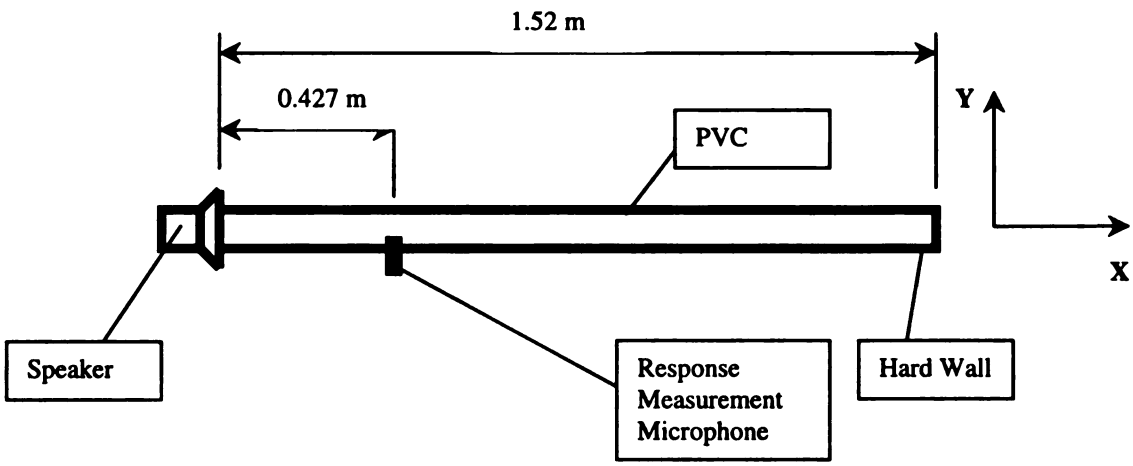

Figure 2 Laboratory Setup for End Pressure Excitation Experiment

The setup used a 76 mm circular PVC schedule 40 duct, 1.52 m long, driven by a 254 mm diameter speaker as sketched in Figure 2. The response of the tube was measured in the experiment with a microphone at a location (x,y)=(0.4267,0.0037). The natural frequencies for this setup can be obtained analytically solving the wave equation. In this particular case, since no internal damping has been assumed, the ideal standing wave response resulting from a reflective boundary condition is infinite at a natural frequency

$$w_n = \frac{n\pi c}{L}$$

where c= 321.4 [m/s], L=1.524 [m] and $n=0,1,2,\ldots$

Each value of n represents the normal mode of vibration with the natural frequency determined from the equation. The theoretical calculations for evaluating the natural frequencies at different mode shapes were performed and shown in Table 1

Table 1 Analytical Natural Frequencies for the Setup

Mode	Frequency [Hz]
1	0
2	105.45
3	210.89
4	316.34
5	421.78
6	527.23

These results will be used to compare the accuracy of the results obtained from the finite element model. The finite element model has the same dimensions as in the experiment, as well as the same boundary conditions.

A schematic for the finite element model is shown in Figure 3

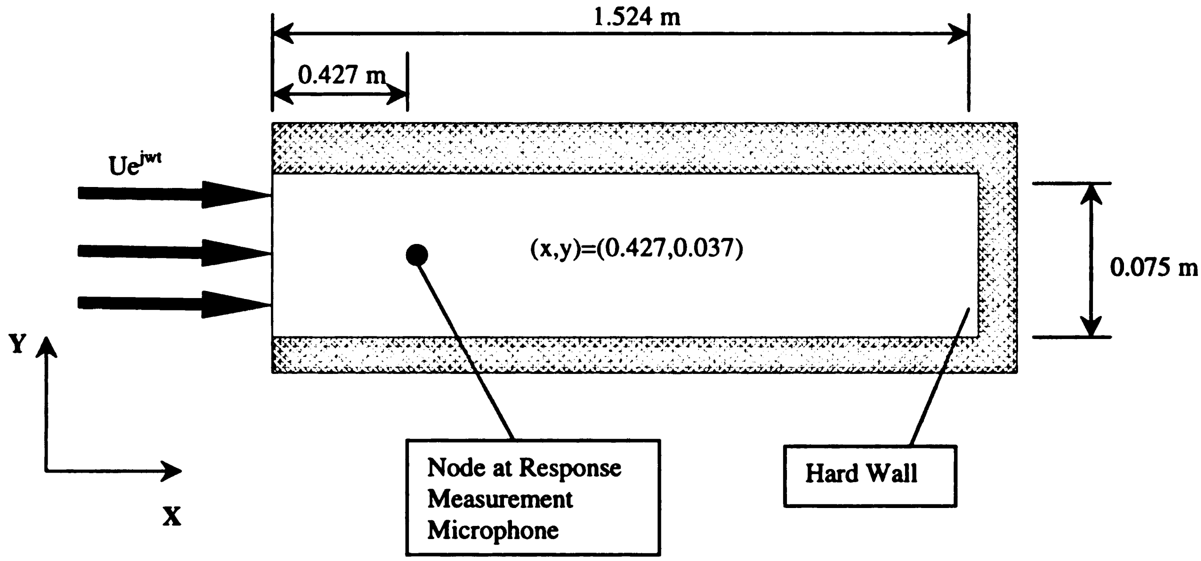

Figure 3 Finite Element Model for the Experiment

Since the speaker acts as a piston in the setup, the model was defined with a uniform input of volume velocity $U e^{jwt}$ in the open end of the acoustic cavity. The 2D finite element model was discretized using 12 elements in Y direction and, in order to study the convergence of the model, 7, 14, 28, 35 and 42 elements were used along the X direction. All the test cases were performed using rectangular four node elements, with one degree of freedom per node. The values of the absolute pressure at the node, representing the microphone position (0.427 m from the speaker) and a150 Hz forcing frequency are given in Table 2.

Table 2 Absolute Pressure Values for Different Mesh Sizes

Mesh	P [N/m^2] at (0.427, 0.037) [m]
12 X 7	3.231812 e –3
12 X 14	3.151551 e –3
12 X 28	3.131725 e –3
12 X 35	3.130641 e –3
12 X 42	3.130514 e –3

As seen from Table 2 , the solution converges to a pressure about 3.13×10^{-3}[N/m^2], which is roughly reproduced by the 12x28 element mesh. The computational effort required for the analysis with the 12x28 is more moderate as compared to the 12x35 and 12x42 element meshes, with a good accuracy. Therefore, the 12 x 28 element mesh is sufficient for this work and will be used to perform further analyses. Based on this mesh, the natural frequencies are shown in Table 3, proving once more that the finite element model is in good agreement with analytical results shown in Table 1.

Table 3 Natural Frequencies from the finite element model

Mode	Frequency [Hz]
1	0
2	105. 39
3	210. 45
4	314. 84
5	420.25
6	525.20

The finite element analysis was conducted for the range of 0 to 800 Hz as described by A. J. Hull [10] and at (x,y)=(0.427,0.037), the output from the finite element model is shown in Figure 4. The position for the measurement is chosen to coincide with the experimental results from [10]. This experimental results will be used later in the analysis to compute values for damping coefficients α and β.

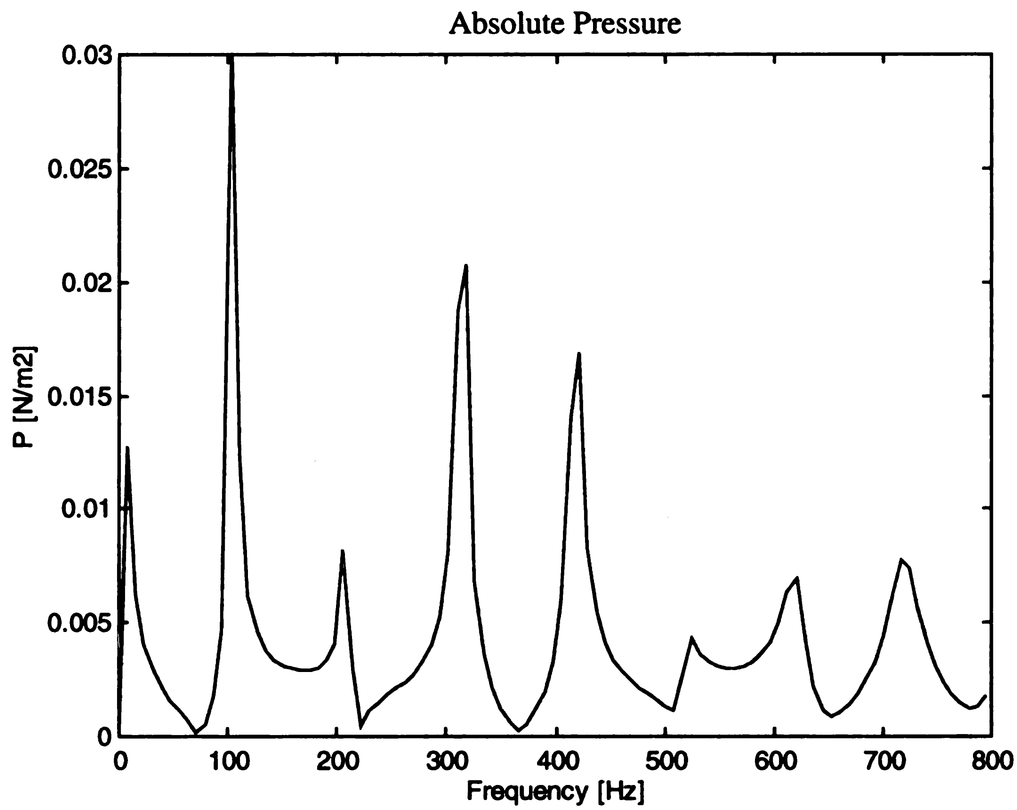

Figure 4 Frequency Response from the Finite Element Model

CHAPTER 3

MODELING POROUS ABSORPTION MATERIAL

3.1 Rigid Porous Absorbing Material

The model of the absorption material is based on the classical theory given by Zwikker and Kosten [7] and Morse and Ingard [8]. For the ideal foam, it is assumed that the material is rigid and therefore, it does not move with the air. The absorption then arises from the viscous forces acting at the air-solid interface and not from any damping within the material itself. At a microscopic level, the flow through the pores is extremely complicated, as the velocity varies across the section. Because of this, an isotropic material is assumed and the governing equations are written in terms of the mean velocity, based on the equations derived for propagation through a narrow tube (Figure 5).

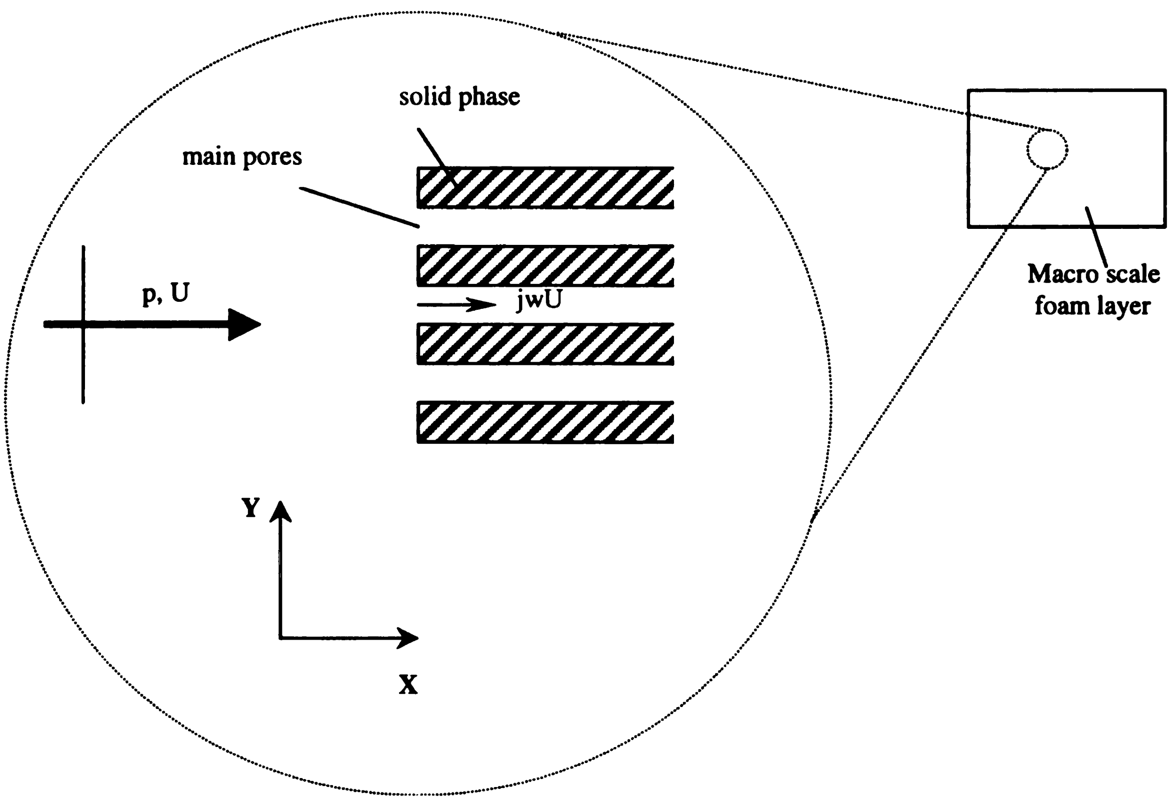

Figure 5 Exaggerated cross-sectional view of a foam layer with oriented interface

In the present theory there are three important physical properties that will influence the absorption: porosity Ω, structure factor K and flow resistivity R. It is also important to understand the concept of main pores for the ideal foam, which are uninterrupted microscopic tubes that cross the entire foam (real foams are also composed by non-communicating air gaps). If there are *n* parallel main pores of radius r distributed over a cross section of unit area, porosity can be written as $n\pi r^2$ and usually varies from 0.80 (wood-fiber plates) to 0.95 (felt, sponge rubber) as tabulated in reference [7]. In the equation of motion, porosity also can be taken as the volume of air in the main pores per unit of volume of foam. The structure factor K is equal to the ratio of the total air contents to that of the main pores, and is essentially greater than1, usually from 3 to 9. The example shown in Figure 5 has structure factor equal to 1, since there are only main pores and they are oriented with the same direction as the macroscopical pressure-gradients. Resistivity is known as the characteristic impedance or resistance of the foam and varies from 2500 to 50000 [rayls/m]. Also in this section, absorption effects are introduced by making the assumption that the lining is locally reacting, since the sound velocity in this medium is two or three times smaller than in air. The advantage of this approach is that the lining can be represented without having to increase the number of degrees of freedom and the finite element method can be applied to model the absorption material as well as the air. This will also have the added advantage of allowing the material lining to have an irregular geometry.

3.2 Equations for a Porous Medium

In this section, equations are derived from a generalized Rayleigh model of material as given by Morse and Ingard [8]. It is assumed that the material is isotropic and the solid phase is rigid. The effect of the material on the entrapped air is considered by introducing the porosity Ω. It is assumed that the input is of the form e^{jwt}, in which case the equation governing the acceleration of the fluid through the pores is

$$\nabla . U = \frac{-jw\Omega}{\rho_0 c_a^{\ 2}} p \tag{9}$$

Continuity requires that

$$-\nabla p = (jw\rho_a + R\ )U \tag{10}$$

where U is the mean velocity of fluid passing through the pores, c_a is the speed of propagation and ρ_a is the effective density of the air inside the pores, defined as

$\rho_a = \rho_0 K$

If U is eliminated from (9) and (10) then the governing equation may be expressed as

$$\nabla^2 p - \left(\frac{w}{c}\right)\left[\left(\frac{w}{c}\right)K\Omega - j\left(\frac{R_e \Omega}{\rho_0 c_a}\right)\right]p = 0 \tag{11}$$

Comparing (11) with (4), we recognize that the behavior of the absorption material is similar to that for air, but includes the effects of resistivity, porosity and structure factor, as postulated in reference [11]. The discretized form of the equation (11) equivalent to (7) for air alone is

$$\{[S\ ]-[P_m]\}\{p_m\}=(j\,\rho\,w+R)\{Q_m\} \tag{12}$$

where Q_m is the volume velocity, [S] is as before and [P_m] is the global dynamic matrix, obtained from the assembly of the element matrices

$$(P_m)_{ij}=\left[\left(\frac{w}{c}\right)^2 K\,\Omega+j\left(\frac{w}{c}\right)\left(\frac{R\,\Omega}{\rho\,c}\right)\right]\int_e N_i N_j dA$$

This matrix is valid also in the limit where the porosity approaches 1, the structure factor approaches 1, and the resistivity approaches zero, which coincide with the analysis of air alone, equation (7). When air and absorption systems are linked together it is assumed that there is a small volume of incompressible fluid at each node point in the connection and further that the dimensions of this volume are small compared with the wavelength.

3.3 Validation and Results for the Coupled Model Air-Foam

To validate the finite element model as well as the coupling procedure between air and foam elements, the experiment conducted by A. J. Hull [10] is now modeled. In his work, Hull built a system model as of a one-dimensional hard-walled duct, excited by pressure input at one end and a partially reflective boundary condition at the other end represented by a complex boundary impedance. The partially reflective condition in the duct allows some energy to be dissipated at the end while the rest is reflected back into the system. The system used a 0.0762 circular PVC schedule 40 duct that was 1.524 m long driven by a 0.254 m diameter speaker. The impedance of a piece of 57 mm thick packing foam inserted in the termination end was tested. Speaker input pressure was measured in the exit plane of the input speaker with a half inch microphone (input reference microphone) attached to a digital signal analyzer. The response of the tube was measured at 0.427 m with another microphone (response measurement microphone) attached to the signal analyzer. This experiment, used as a reference for the validation of the finite element approach is sketched in Figure 6

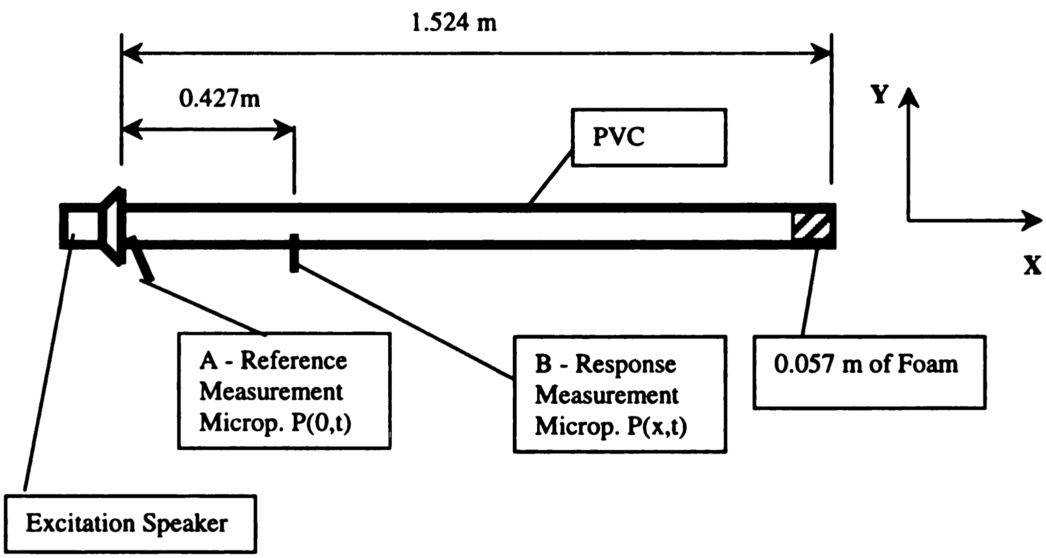

Figure 6 Laboratory Setup for End Pressure Excitation Experiments

The finite element model used is sketched in Figure 7. The 2D mesh was built using 12 elements along the Y direction and 28 elements along the X direction, as suggested by the analysis in Chapter 2 . Elements are rectangular with one degree of freedom per node.

The finite element model is sketched in Figure 7

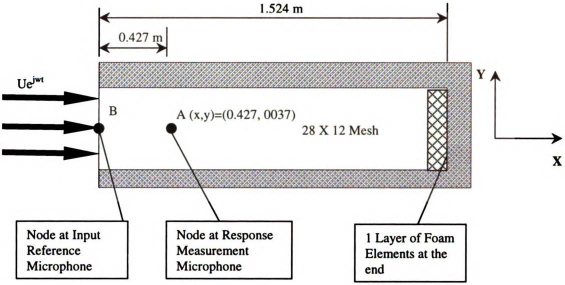

Figure 7 Finite Element Model for the Laboratory Setup

The volume of air is excited by a volume velocity field $Q = j\rho\omega U$.

The results from the finite element model are shown in Figures 8, 9, 10 and 11. Figures 8 and 9 show the ratio of absolute pressure at A ((x,y)=(0.427, 0.037)) to absolute pressure at B ((x,y)=(0, 0.037)) for the finite element model and experiment, respectively. Figures 10 and 11 show the phases differences at the same locations, also for the finite element model and experiment. Results in Figures 9 and 11 also show the analytical results for the experiment based on a mathematical model of a long, thin duct with a speaker at one end and a partial reflective termination end, as discussed in [10].

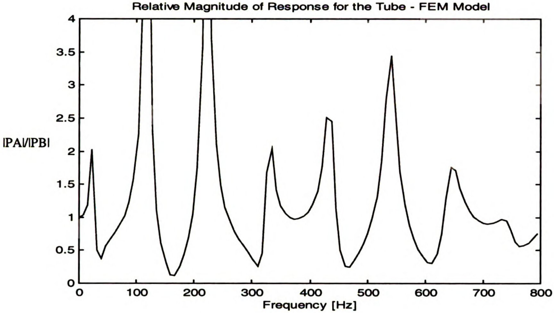

Figure 08 Frequency response of duct with foam - F.E. Model

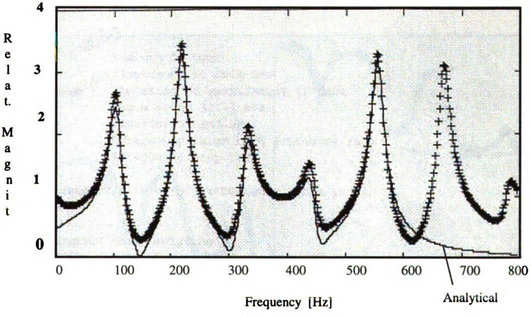

Figure 09 Frequency response of a duct with foam - Experiment

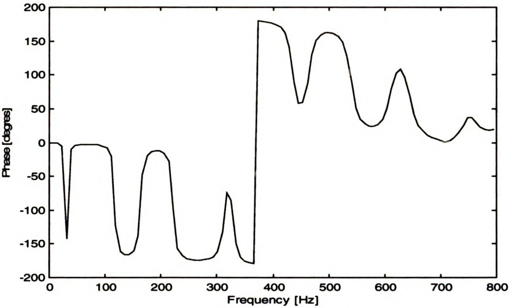

Figure 10 Phase Difference between input and measured response - F.E. Model

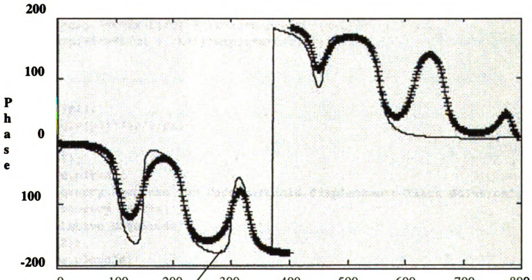

Figure 11 Phase Difference between input and measured response - Experiment

The accuracy of the simulated finite element model can be seen comparing Figures 8, 9, 10 and 11, where the relative magnitude of absolute pressure as well as the phase angle closely match the experimental and analytical results. At this point, the output from experimental data is used to define the values of damping coefficients (α and β) for the finite element model. Since the foam at the end was modeled with the same characteristics as in the experiment, it is assumed that the same level of damping relative to the foam is transferred to the cavity. The extra damping necessary to make the response of the finite element model match the experiment is obtained setting

$$\alpha=(w/c)^{-2}*0.000001 \quad \text{and} \quad \beta = 0.000001.$$

Since the FEM model has been formulated and validated for a range of frequencies, we will now proceed to analyze the influence of different shapes of foam in the reduction of noise in the acoustic cavity.

CHAPTER 4

ANALYSIS AND RESULTS

4.1 Analysis and Results for Different Shapes of Foam

In this chapter we demonstrate the potential utility of the foam finite element model to explore the influence of the shape of a layer of foam on the response of the system.

To study this problem, the same geometry as used in the experiment by A. J. Hull [10] is used to model the finite element problem, but now with an extra extension at the end of the tube which will be filled with foam in layers of different shapes.

This extension was 0.381 [m] long with the same diameter (0.075 [m]) as the PVC tube and was discretized using 12 elements in the width (Y) and 7 elements in the length (X) direction. The objective is to analyze the influence of different shapes of foam layers, keeping the dimensions of the extension constant. This geometry is shown in Figure 16

A wide variety of foam material is commercially available such as polypropilene, polystirene, fiber glass, each having different properties. Typically, resistivity varies from 2500 up to 50000 [Rayls/m], porosity from 0.5 up to 0.95 , structure factor usually from 3 to 9 and densities from 6 up to 30 [$^{Kg}/m^3$]. In the present model we perform the analysis just using a particular type of foam, since the goal is not to analyze the influence of different properties of the foam materials, but instead to study the effect of different layer geometries of the same type of foam. The present analysis has been performed with a foam of the type of Polyurethane Flexible with the following characteristics:

resistivity =2500 [Rayls/m]   porosity = 0.9   density = 6 [Kg/m^3]   Structure factor=2

This foam is the most common which is economical and easy to use. The finite element for the model with extension is sketched in Figure 12.

Figure 13 shows the arrangement in scale and different geometries of the foam layer.

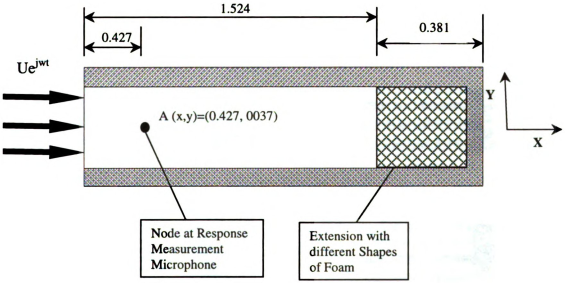

Figure 12 Finite Element Model for the variation of the laboratory setup

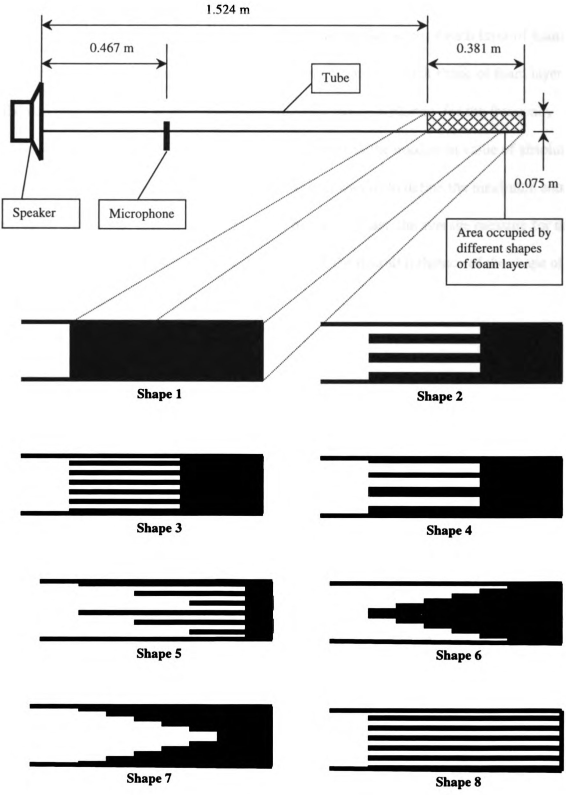

Figure 13 Different shapes of foam layer analyzed

In the following section we shall study the efficiency of each foam layer shown in Figure 16 on the reduction of noise. In order to evaluate the performance of each layer of foam, three performance parameters where used. In the first one, for each shape of foam layer, the maximum value of absolute pressure inside the cavity is plotted for the frequency range from 0 to 800 Hz. The second parameter measures the maximum value of absolute pressure for each shape in ranges of 100 Hz. This allows us to define the maximum sound pressure level in the cavity for each range of frequency. Last, the average pressure for the cavity for the range frequency of 0 to 800 Hz gives the overall influence of the shape of foam layer in the reduction of noise level.

1 – Maximum Absolute Pressure

We computed the maximum values of absolute pressure for input frequencies ranging from 0 up to 800 [Hz]. These values are independent of the location in the acoustic cavity. This can be mathematically represented as

$$\Phi_1(w) = \max_{(x,y)\in\Omega_{air}} \| p_w(x,y) \|$$

where $|p_w|$ is the absolute pressure in the acoustic cavity as a result of a periodic excitation at frequency w.

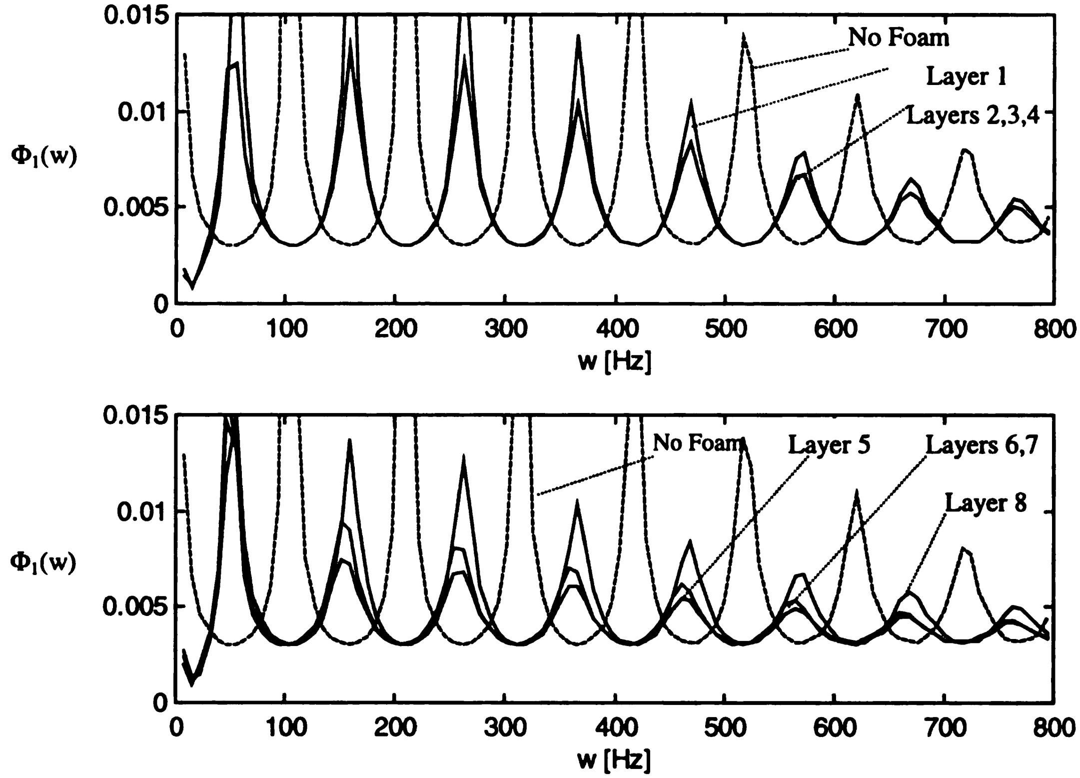

Figure 14 Maximum absolute pressure for each shape of foam layer

Figure 14 shows that when foam is added, peaks in the response are shifted to the left, indicating the effect of damping introduced by the foam. Comparing results for the different shapes, we observe that shapes 5, 6, 7 show a substantial decrease in the pressure values. Table 4 shows the maximum absolute pressure for frequencies in different ranges.

Table 4 Maximum Absolute Pressure for Input frequencies in Different Ranges

Maximum Absolute Pressure in Range [10^{-4} N/m^2]									
Range	**Shape of Foam Layer**								
[Hz]	**No Foam**	**1**	**2**	**3**	**4**	**5**	**6**	**7**	**8**
0~100	129.34	230.13	124.77	124.26	124.62	164.95	147.13	147.15	150.07
100~200	520.55	238.85	133.08	132.52	132.89	74.23	94.06	94.05	136.98
200~300	274.81	188.46	125.50	125.00	125.31	68.21	81.03	81.03	125.96
300~400	238.98	139.55	104.05	103.78	103.93	61.13	70.76	70.75	103.85
400~500	182.09	104.28	83.77	83.70	83.72	54.81	61.51	61.52	83.64
500~600	138.94	79.12	67.26	67.34	67.26	49.56	53.29	53.29	67.30
600~700	108.66	65.12	58.07	58.05	58.05	44.79	47.42	47.40	58.04
700~800	77.86	54.58	50.54	50.51	50.52	42.02	43.21	43.20	50.51

From the results it can be clearly seen that we get highest values of absolute pressure for the whole range of frequencies for the case without foam. This suggests that addition of foam, as expected, is an effective remedy for reduction of noise in the acoustic cavity. The maximum pressure values for shapes 2, 3 and 4 are similar. This may be attributed to the fact that the mesh is not sufficiently refined to capture significant differences between the pressure values. Shape 5 seems to be the most cost-effective geometry since it results in minimum pressure levels for all frequencies with 40% less foam applied.

2 – Sound Pressure Level (SPL)

The most widely used method in the field of acoustics to measure accurately the noise intensity in an acoustic cavity is the sound pressure level (SPL). It relates the measured absolute pressure with the quietest sound that can be heard by the average person. The mathematical formulation is shown.

$$SPL = 20\log_{10}\left(\frac{T}{20x10^{-6}}\right)[dB]$$

where

$$T = \max_{w \in Range_i}\left[\max_{(x,y)\in\Omega_a} |p_w(x,y)|\right]$$

and

$$Range_{i=1,\dots,8} = [(i-1)*100, i*100]$$

The values of sound pressure level for different layers of foam have been plotted as shown in figure below, using the frequencies range in Table 4.

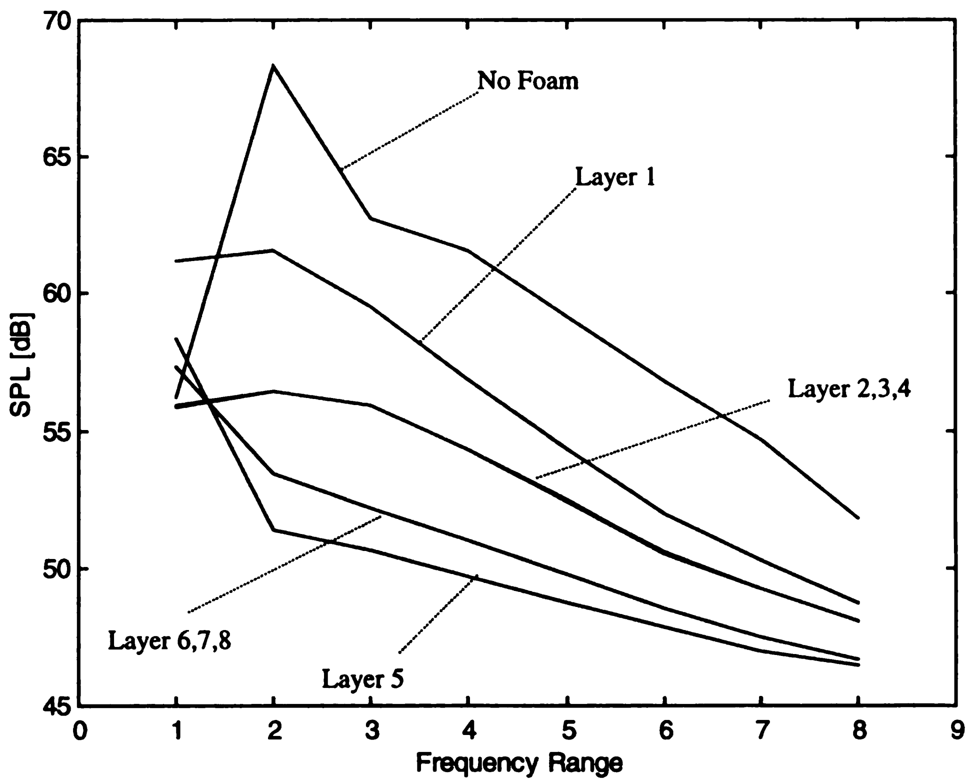

Figure 15 Sound Power Level for each shape of foam layer

Again, Figure 15 shows that shape 5 shows the maximum amount of reduction in noise level throughout the acoustic cavity for the entire range of frequencies

3- Average Pressure

This function Φ_2 averages the overall behavior of the acoustic cavity for all frequencies.

$$\Phi_2 = \int_0^{800} \int_{\Omega_{air}} \| p_w(x,y) \| dA\, dw$$

The results for each layer are shown in Table 5

Table 5 Average Pressure for each Layer of Foam

Layer of Foam	Φ_2 [N/sec]
No Foam	3.481×10^5
1	3.092×10^5
2	2.906×10^5
3	2.905×10^5
4	2.906×10^5
5	2.687×10^5
6	2.739×10^5
7	2.740×10^5
8	2.909×10^5

This performance measure again shows that layer 5 is the most efficient and effective use of foam material.

The ratio of the performance Φ_2 of each layer of foam with respect to a no foam design is shown in Figure 16.

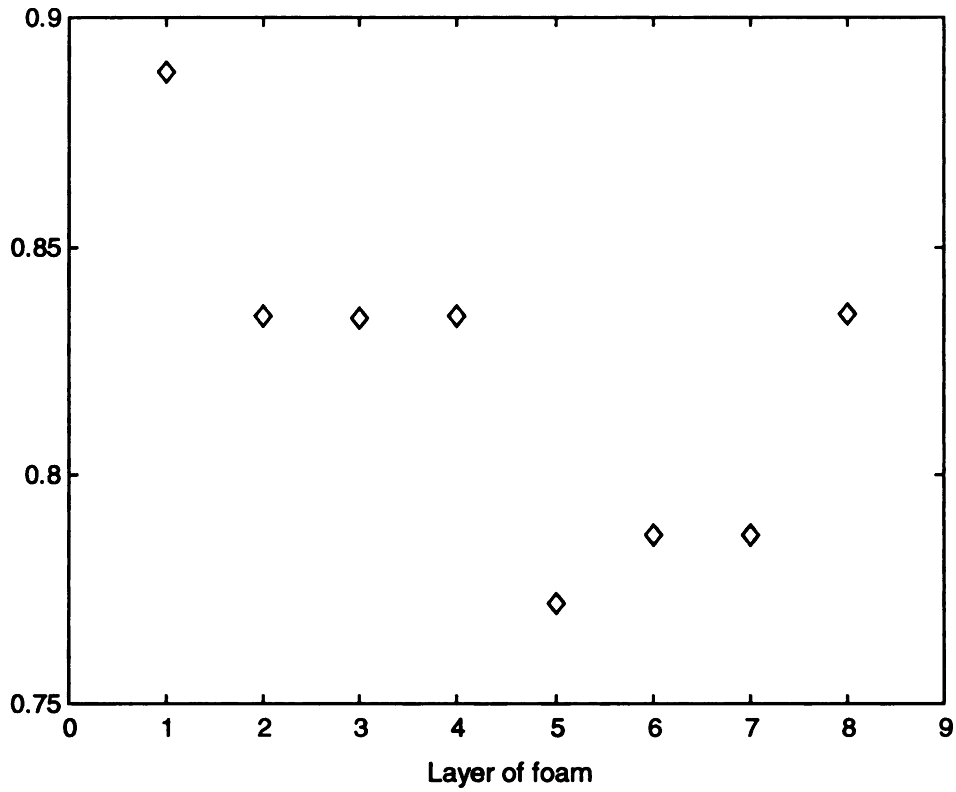

Figure 16 Average pressure for each shape of foam layer

Figure 16 again verifies the superiority of shape 5. It also shows that shapes 6 and 7, which have reasonably low ratios are good options. Although the use of more material involved in these shapes may increase costs, ease of manufacturing may compensate and, overall, shapes 7 and 8 may turn out to be comparable to shape 6 in terms of cost-efficiency.

CHAPTER 5

CONCLUSIONS

In this work we have formulated a finite element model to study the influence of foam treatment in the reduction of noise level. Early work in this field by Craggs followed the same approach to evaluate the performance of reactive mufflers. However, Craggs implemented his model only for a planar foam geometry, analyzing foams with different physical properties such as resistivity and porosity. In this study, we developed a finite element model based on Craggs' technique and analyze the model for different foam geometries keeping the physical properties of the material constant. In addition, we explored the relation between the shape of the foam layer and the reduction of noise level in an acoustic cavity. In order to verify the accuracy and efficiency of the model, a comparative study was made with analytical and experimental results. This study shows that the results obtained from our model closely match with experimental results, thus proving the validity of the model.

The results show that the sound pressure level in an acoustic cavity can be reduced with addition of foam material in a restricted volume inside the cavity. This reduction is related more to the shape of lining , than to the amount of foam material used, with better results found for shape of foams (Figure 13) with 30% to 40% less absorption material than the same restricted volume full of foam. The results suggested that the reduction of sound pressure level in the cavity with foam is of the order of 10 dB (Figure 15) for shapes 5, 6, 7 in some range of frequencies. This physically represents a noise level, which is half the original noise in the cavity without foam, and it is clearly perceptible to the human hearing.

Factors not addressed in this thesis are the investigation of non isotropic foams and different properties such as resistivity and tortuosity. Future topics should include this analysis as well as the setup of the experiment in order to validate all the results from the finite element model.

APPENDICES

APPENDIX A

A Subroutine for input the general characteristics of the acoustic cavity and foam

```
%General characteristics for Acoustic Cavity and Foam
format long

% This program  works for Rectangular elements with 1 dof per node

% Data shared with FEM program

global  ynumbel+1 numel numfix numload bigstif ndf neqs neqm gieq ieq…
jeq condu plate rayls xbe xpla connec fixlist loadlist loadval density…
alfa tknel gjeq eqden omgi ps sk vecfoam percred nodref cnfo elefo…
fobet foalf presec premic resinc rowsp pk force disp pknel lnel anel…
xnel numel nel coun inel psnel pcsnel pisp ms cs numnopla  xdimens…
xnumbel freqmed pcs mz numepl passo connecpl betad omgf capac leng timet
alfafo betafo vecbeta vecalfa rowsbot

ndf=1;

% Medium characteristics
ydimens=input('Width of the Medium [mm]');
ynumbel=input('Number of elements in Y direction');
xdimens=input('Length of the Medium [mm]');
xnumbel=input('Number of elements in X direction');
rowsbot=input('Length of the extension [mm] );
xdimens=(xdimens+correc)/1000;%input('Lenght of the Medium');
rowsbot=floor(rowsbot/(xdimens/xnumbel));
xnumbel=xnumbel+rowsbot


% Data for a particular example

numepl=xnumbel*ynumbel; %number of elements in the medium
numnopla=(xnumbel+1)*(ynumbel+1);
elefo=zeros(1,numepl);
numfix=5;
numload=ynumbel+1;
bigstif=0;
xpla=zeros(2,numnopla);
connecpl=zeros(4,numepl);

nodepress1=(.43688/(xdimens/xnumbel));
premic=numnopla-(floor(nodepress1)*ynumbel+1)-((ynumbel+1-1)/2)
diferposit=.43688-(floor(nodepress1)*(xdimens/xnumbel))
lastel1=numepl-(floor(.43688/(xdimens/xnumbel))*numel);
row_after_mic=lastel1-numel+1:lastel1

nodepress2=(.69088/(xdimens/xnumbel));
presec=numnopla-(floor(nodepress2)*ynumbel+1)-((ynumbel+1-1)/2)
lastel2=numepl-(floor(.69088/(xdimens/xnumbel))*numel);
row_behind_secp=lastel2-numel+1:lastel2

rob=(lastel1+lastel2)/2;
row_between=rob-numel+1:rob
pause
foalf=zeros(1,numepl);
fobet=zeros(1,numepl);
vecfoam=zeros(1,numepl);
chekfo=(1:numepl);
resimet=2500;%[Resistivity in rayls/meter]
resinc=resimet;
resit=(resinc);
```

```
pors=.9;%Porosity
tort=2;%Tortuosity (Structure Factor)

typefoam=input('None    (1)      Botton(2)   Wall(3)      Botton+Wall(4)
Triang.@Botton(5) Randon(6)  Begin(7)=')'

if(typefoam==1) %None
   vecfoam=zeros(1,numepl);
end

if(typefoam==2) %Botton
   row=rowsbot%input('How many rows of foam @ Botton ?')

   row=1

   rowsp=row
   vecfoam=zeros(1,numepl);
   for ty=1:row*numel
      vecfoam(ty)=1;
      foalf(ty)=pors*resit
            fobet(ty)=tort*pors;
            chekfo(ty)=0;
   end

end

if(typefoam==3) % Wall
   row=input('How many rows of foam in the Wall ?')
   vecfoam=zeros(1,numepl);
   wall=numel;
   while(wall<=numepl)
   for ty=1:row
      vecfoam(ty+wall-numel)=1;
      vecfoam(wall-ty+1)=1;
      foalf(ty+wall-numel)=pors*resit;
            fobet(ty+wall-numel)=tort*pors;
            foalf(wall-ty+1)=pors*resit;
            fobet(wall-ty+1)=tort*pors;
   end
   wall=wall+numel;
   end
end

if(typefoam==4)% Botton and wall
   row=input('How many rows of foam in the Wall and Botton ?')
   vecfoam=zeros(1,numepl);
   for ty=1:row*numel;
      vecfoam(ty)=1; %Apply at the Botton
   end
   wall=numel*(row+1);

   while(wall<=numepl)
   for ty=1:row
      vecfoam(ty+wall-numel)=1;  % Apply left wall
      vecfoam(wall-ty+1)=1;      % Apply right wall
   end
   wall=wall+numel;
   end
end

if(typefoam==5) % Triangular @ Botton
```

```
   row=input('How many rows of foam at Botton ?');

   vecfoam=zeros(1,numepl);
   if(row>1)
     for ty=1:row*numel
      vecfoam(ty)=1; %Apply at the Botton
      foalf(ty)=pors*resit;            fobet(ty)=tort*pors;
     end
   end
   wall=numel*(row+1);

   rat=numel/2;
   con=1;
   while(con<rat)
   for ty=1:rat-con
      vecfoam(ty+wall-numel+con)=1; % Apply left wall
      vecfoam(wall-ty-con+1)=1; % Apply right wall
      foalf(ty+wall-numel+con)=pors*resit;
           fobet(ty+wall-numel+con)=tort*pors;
           foalf(wall-ty-con+1)=pors*resit;
           fobet(wall-ty-con+1)=tort*pors;
           ty=ty;
           con=con;

   end
   con=con+1;
   wall=wall+numel;

   end
end

if(typefoam==6) % Randon
bata=pors*tort;
casel=input('Which Case to study ?');

if (casel==1) % 7 rows Full at Botton
nufiel=7*12;%Total of foam elements
vecapf=[1:84];%Vector with applyed foam
end

if (casel==2) % Thick toot
nufiel=60;%Total of foam elements
vecapf=[1:36,39:4:83,40:4:84];%Vector with applyed foam
end

if (casel==3) % Thin toot
nufiel=60;%Total of foam elements
vecapf=[1:36,38:2:84];%Vector with applyed foam
end

if (casel==4) % Irregular toot
nufiel=60;%Total of foam elements
vecapf=[1:36,37:12:73,40:12:76,43:12:79,44:12:80,47:12:83,48:12:84];%Vec
tor with applyed foam
end

if (casel==5) % Dif. lenght toot
nufiel=36;%Total of foam elements
vecapf=[1:12,13:2:35,37:6:79,39:6:57]%Vector with applyed foam
pause
end
```

```
if (casel==6) % Triangular
nufiel=54;%Total of foam elements
vecapf=[1:24,26:35,39:46,52:57,65:68,78:79];%Vector with applyed foam
end

if (casel==7) % Triangular Invert
nufiel=54;%Total of foam elements
vecapf=[1:24,25:29,37:40,49:51,61:62,73,32:36,45:48,58:60,71:72,84];%Vec
tor with applyed foam
end

if (casel==8) % Long teet
nufiel=42;%Total of foam elements
vecapf=[2:2:84];%Vector with applyed foam
end

if (casel==9) % 1 Row in the middle - For T.Loss only
nufiel=8;%Total of foam elements
vecapf=[136:143];%Vector with applyed foam
end
       for kr=1:nufiel
         numbel=vecapf(kr)

         fobet(numbel)=bata;%input('Beta value for the element ?');
         foalf(numbel)=pors*resit/(150*1.21);%(13386*4.344e-5);
         vecfoam(numbel)=1; % Apply foam in the element
         chekfo(numbel)=0;  % Show which element

       end % for elements
end
%vecfoam(1:96)
pause

if(typefoam==7) %Beggining of the medium
   row=3;%input('How many rows of foam @ Begin ?')
   vecfoam=zeros(1,numepl);
   for ty=(numepl-row*numel+1):numepl
      vecfoam(ty)=1;
   end

end



% Nodal coordinates based on nodal definition

yposi=xdimens;
cont=1;

for k=1:numnopla;

   xpla(1,k)=xbe(1,cont);
   xpla(2,k)=yposi;

   if(cont==ynumbel+1);
      yposi=yposi-(xdimens/xnumbel);
      cont=0;

   end
```

```
cont=cont+1;

end

contel=0;
con=1;
tkel=1;
dens=1.21;
alf=0.000001;
bet=0.000001;

% Element Conductivity
condu=[321.4,0;0,321.4;]';

for k=1:numepl;

% Element connectivity definition
%connec=[1,2,5,4;2,3,6,5;4,5,8,7;5,6,9,8]'
   connecpl(1,k)=contel+k+ynumbel+1;
   connecpl(2,k)=contel+k+ynumbel+1+1;
   connecpl(3,k)=contel+k+1;
   connecpl(4,k)=contel+k;
   elementonaconnc=k;
   connecpl(1:4,k);
   con=con;
   contel=contel;
   %pause

   if(connecpl(3,k)/ynumbel+1==con)
      contel=contel+1;
      con=con+1;
   end

% Tickness
   tknel(k)=tkel;



% Element Density

   density(k)=dens;

% Element alfa & beta (alfaXmass matrix and betaXstiffness matrix)
   alfa(1,k)=alf;
   alfa(2,k)=bet;

end

% Medium equilibrium Density
dens=1.21;
eqden=1.21;
% Medium Speed of sound
capac=321.4;

% Adiabatic Bulk modulus
betad=20.55172;% lbf/in2 or 141700 N/m2

% Areas
areas0=[5;5;5;5];
```

```
% Total number of equations
neqm=numnopla*ndf;

% One  single FEM evaluation

[f0,g]=trufoam(areas0);

rayls=2500;
betafo=1;
alfafo=2500

cnfo=0;%Number of elements in the medium that are foams

for ke=1:numepl % Select only foam elements
   if(vecfoam(ke)==1)
   cnfo=cnfo+1;
   elefo(cnfo)=ke; %vector with wich element is foam

   end
end
```

APPENDIX B

Subroutine for global matrix assembly and solution of the equations

```
function[f,g]=trufoam(areas0)

% Data shared with main program

global ynumbel+1 numel numfix numload bigstif  ndf neqm condu betad...
pisp eqden passo pcs fnodal xpla connec connecpl fixlist loadlist... force
neqs loadval density alfa tknel omgi omgf pk ps pk  disp... numnopla ms cs
sk vecfoam pknel psnel pcsnel lnel anel gieq gjeq...
ieq jeq xnel numepl nel mz leng ynumbel fobet foalf presec premic...
resinc rowsp ydimens rowsbot

resinc=resinc
pk=zeros(neqm,neqm);
ps=zeros(neqm,neqm);
pcs=zeros(neqm,neqm);
pfk=zeros(neqm,neqm);
pfsa=zeros(neqm,neqm);
pfsb=zeros(neqm,neqm);
pfcs=zeros(neqm,neqm);
flux=zeros(numnopla,1);
disp=zeros(neqm,1);
zisp=zeros(neqm,1);
relat=zeros(neqm,1);
mbig=zeros(neqm+neqs,neqm+neqs);
bcon=zeros(neqm,neqs);
pknel=zeros(4*ndf,4*ndf);
psnel=zeros(4*ndf,4*ndf);
pcsnel=zeros(4*ndf,4*ndf);
xnel=zeros(2,4);
fobeta=1;
foalfa=1;% for alfa and beta values when medium alone
for nel=1:numepl;
gera=1;
passw=0;


if(vecfoam(nel)==1)
   density(nel)=6;
   passw=1;
   fobeta=fobet(nel);
   foalfa=foalf(nel);

end

% Information about element "nel" of the medium
elemento=nel;
node1=connecpl(1,nel);
node2=connecpl(2,nel);
node3=connecpl(3,nel);
node4=connecpl(4,nel);
xnel(1,1)=xpla(1,node1);
x1=xpla(1,node1);
xnel(2,1)=xpla(2,node1);
y1=xpla(2,node1);
xnel(1,2)=xpla(1,node2);
x2=xpla(1,node2);
xnel(2,2)=xpla(2,node2);
xnel(1,3)=xpla(1,node3);
xnel(2,3)=xpla(2,node3);
xnel(1,4)=xpla(1,node4);
```

```
xnel(2,4)=xpla(2,node4);
y2=xpla(2,node4);
alfel=alfa(1,nel);
betel=alfa(2,nel);
dnel=density(nel);
tnel=tknel(nel);

% Build element matrix pknel

sknel=trusspl(xnel,anel,dnel,tnel,alfel,betel,condu);

% Assemble the element matrix into
% global stiffness matrix pk

for k=1:4;
nodei=connecpl(k,nel);
for idof=1:ndf;
ieq=(k-1)*ndf+idof;
gieq=(nodei-1)*ndf+idof;
for j=1:4;
nodej=connecpl(j,nel);
for jdof=1:ndf;

jeq=(j-1)*ndf+jdof;
gjeq=(nodej-1)*ndf+jdof;

%Mounting matrices for connection medium + foam

% Creates foam matrix alone
if (passw ==1) %

pfk(gieq,gjeq)=pfk(gieq,gjeq)+(pknel(ieq,jeq));
result=pknel(ieq,jeq);
pfsa(gieq,gjeq)=pfsa(gieq,gjeq)+(psnel(ieq,jeq));
pfcs(gieq,gjeq)=pfcs(gieq,gjeq)+(pcsnel(ieq,jeq));
end

% Creates medium matrix alone
if (passw ==0)
pk(gieq,gjeq)=pk(gieq,gjeq)+pknel(ieq,jeq);
ps(gieq,gjeq)=ps(gieq,gjeq)+psnel(ieq,jeq);
pcs(gieq,gjeq)=pcs(gieq,gjeq)+pcsnel(ieq,jeq);
end

end
end
end
end
end

% Eigenvalues
%tem=eig(pk,ps);
%tem=sqrt(tem);
%tem=sort((tem))/(2*pi);
%for k=1:neqm
%k=k
%tem(k)
%pause
%end

% Solve Harmonic function
```

```
cnt=1;
esp=1;
ploto=10;

cnt=1;

analysis=1;% (1) Frequency for a given node  (2) Pressure for a given
flux=zeros(numnopla,1); % flux vector
veloc=6.2e-9;
for k=numnopla-ynumbel+1+1:numnopla-1

   flux(k,1)=veloc; % Apply speaker effect at the  start

end



fomid=numnopla-(ynumbel+1*5)-((ynumbel+1-1)/2);

%while wf>0

%_________________________________ Pressure _________________________

if(analysis==2)
wf=10;
while wf>0
tyeste=2
wf=input('Initial Frequency');

   %Change next equation to return to the original problem
foa=((((wf/321.4)^2))*pfsa)+((i*wf/321.4)*pfsa*(foalfa))+(pfk);
foa=foa*((i*eqden*wf)/(i*eqden*wf+(resinc)));
med=((-((wf)^2))*ps)+(i*wf*pcs)+(pk);%/eqden/betad

   a=foa+med;
   d=flux*(i*eqden*wf);
   f=a\d;
   sum=0;
   conti=1;
        for col=1:neqm;
   disp(cnt,col)=abs(f(col));%/(321.4*eqden);
   end
   premic
   pres_mic=f(premic)
   pres_mic=disp(1,premic)
   pres_beh=disp(1,presec)
end
end

%_________________________________ Frequency _________________________
if(analysis==1)
sumger=0
omgi=input('Initial Frequency');
omgf=input('Final Frequency');
passo=input('Passo');

for wf=omgi:passo:omgf
wf=wf
ymaxi=0;
ymini=10;
```

```
sum=0;

%__________________ Proposed by Craggs K X M matrices ________________-

   %Change next equation to return to the original problem

foa=((-((wf/150)^2))*pfsa*fobeta)+((i*wf/150)*pfsa*(foalfa))+(pfk/4);
foa=foa*((i*eqden*wf)/(i*eqden*wf+(resinc)));
med=((-((wf)^2))*ps)+(i*wf*pcs)+(pk);%/eqden/betad

   a=foa+med;
   d=flux*(i*eqden*wf);
   f=a\d;
   sum=0;

   lowli=(rowsbot+1)*ynumbel+1;% Define the valid nodes out from foam
        for col=1:neqm;

   disp(cnt,col)=abs(f(col));%abs(f(col));%Absolute Pressure
   zisp(cnt,col)=(f(col));



   check=rowsbot*ynumbel+1;
   if(cnt>1)
     if(col>lowli)
       sum=sum+disp(cnt,col);
     end
   end

   end % for col

   if(cnt>1)
    maxreal(cnt)=max(real(zisp(cnt,lowli:neqm)));%max real of each
frequency
    maximag(cnt)=max(imag(zisp(cnt,lowli:neqm)));%max imag of each
frequency
    maxabs(cnt)=max(disp(cnt,lowli:neqm));%max absolute value of each
frequency
   end

   sumger=sumger+(wf*sum);
   cnt=cnt+1;
end %for frequency
end %Analysis 1
%________________ Max Max real, Imag part and absolute values
maxmxre=max(maxreal)
maxmxim=max(maximag)
maxmsabs=max(maxabs)
performance=sumger
pause
mreal=maxreal'
size(maxreal)
pause
mimag=maximag'
size(maximag)
pause
mabs=maxabs'
size(maxabs)
pause
```

```
wfg=1500/passo;
%for wfg=1:(omgf-omgi)/passo
gnt=1;
   for k=1:ynumbel+1
      for l=1:ynumbel+1
      x(k,l)=[k];
      y(k,l)=[l];
      cel(k,l)=disp((wfg),gnt);
      cnt=gnt+1;
      end
   end
   [X,Y]=meshgrid(x,y);
   surf(x,y,cel)

   title('Pressure Distribution');
   xlabel('col of nodes');
   ylabel('row of nodes');
   modeshape=cel;
   modeshape=modeshape'
   pause

   %axis([1 ynumbel+1 1 ynumbel+1])
   %pause
   contour(x,y,cel)
   pause

ploto=input(' Surf(1)  Frequency/node(2)  or Exit(0)');

%_____________________________ Surf Plot___________________
if(ploto==1)
   gnt=1
   for k=1:ynumbel+1
      for l=1:ynumbel+1
      x(k,l)=[k];
      y(k,l)=[l];
      cel(k,l)=disp(1,gnt);
      gnt=gnt+1;
      end
   end

   size(cel);
   surf(x,y,cel)
   axis([1 ynumbel+1 1 ynumbel+1 ])
   xlabel('row of nodes');
   ylabel('col of nodes');
   zlabel('Pressure');
   title('Wave Pressure Distribution');
   tyu=1;
end
%_____________________________ Frequency Plot  ____________________
if(ploto==2)
node=1000
% Selection and response for a given node
while ploto>0
node=input('Node to plot');
dgof=1;
col=(node);
w_init=omgi
w_finis=omgf
x=omgi:passo:omgf;
```

```
y=1:neqm;
[X,Y]=meshgrid(x,y);
wft=omgi;
for row=1:((omgf-omgi)/passo)+1;
   p(row)=disp(row,col);
   nref=(numnopla-((ynumbel+1-1)/2));
   ph(row)=angle(zisp(row,col)/zisp(row,nref))*(360/2/pi);
   q(row)=(disp(row,col)/disp(row,nref));
end
performance=sumger
xeix=floor((omgi:passo:omgf)/(2*pi));
plot(xeix,q);
axis([0 800 0 4])
relatpre=q;
relatpre=relatpre'
pause
plot(xeix,ph);
axis([0 800 -200 200])
phase=ph;
phase=phase'
pause
plot(xeix,p);
axis([0 800 0 1e-2])
absolpres=p;
absolpres=absolpres'
pause
plot(xeix,20*log10(p/2e-5));
axis([0 800 0 70])
db=20*log10(p/2e-5);
db=db'
pause
   plot(q);
title('Medium  --   Phase Angle');
   xlabel('Frequency [rad/s]');
   ylabel('Phase');
   %axis([omgi (omgf-omgi)/passo 0 4])
   end
end
```

APPENDIX C

Subroutine for the strain energy, kinetic energy and damping matrices of the element.

```
function [pknel]=trusspl(xnel,anel,dnel,tnel,alfel,betel,condu)
global pknel lnel psnel pcsnel tknel capac mz betad eqden
% Make element stiffness matrix: rectangular element
% xnel(1,i):  "x" coordinate of node i. i=1,2
% xnel(2,i):  "y" coordinate of node i. i=1,2
% anel: element area
% enel: element Young's modulus
% dnel: element density
dx=abs(xnel(1,2)-xnel(1,1));
dy=abs(xnel(2,4)-xnel(2,1));
cond1=condu(1,1);
cond2=condu(1,2);
cond3=condu(2,2);
anel=dx*dy;
% Medium Element Stiffness Matrix
eil=tnel;
sx=cond1*dy/(6*dx);
sy=cond3*dx/(6*dy);
pknel(1,1)=2*sx+2*sy;
pknel(1,2)=-2*sx+sy;
pknel(1,3)=-sx-sy;
pknel(1,4)=sx-2*sy;
pknel(2,1)=-2*sx+sy;
pknel(2,2)=2*sx+2*sy;
pknel(2,3)=sx-2*sy;
pknel(2,4)=-sx-sy;
pknel(3,1)=-sx-sy;
pknel(3,2)=sx-2*sy;
pknel(3,3)=2*sx+2*sy;
pknel(3,4)=-2*sx+sy;
pknel(4,1)=sx-2*sy;
pknel(4,2)=-sx-sy;
pknel(4,3)=-2*sx+sy;
pknel(4,4)=2*sx+2*sy;
pknel=pknel*dnel*cond1;
%Medium Element Mass Matrix
mz=anel*dnel/(36);
psnel(1,1)=4;
psnel(1,2)=2;
psnel(1,3)=1;
psnel(1,4)=2;
psnel(2,1)=2;
psnel(2,2)=4;
psnel(2,3)=2;
psnel(2,4)=1;
psnel(3,1)=1;
psnel(3,2)=2;
psnel(3,3)=4;
psnel(3,4)=2;
psnel(4,1)=2;
psnel(4,2)=1;
psnel(4,3)=2;
psnel(4,4)=4;
psnel=mz*psnel;
% Medium Damping Matrix
pcsnel=(alfel*psnel)+(betel*pknel);
```

BIBLIOGRAPHY

[1] Craggs A., " A Finite Element Model for Rigid Porous Absorbing Material", Journal of Sound and Vibration 61(1), 101-111, (1978)

[2] Craggs A., " The Application of Acoustic and Absorption Finite Elements to Sound Fields in Small Enclosures", Finite Element Applications in Acoustics , (1-20), (1981)

[3] Scott R. A., " The Propagation of Sound between walls of Porous Material", Procedings of the Physical Society of London 58(1), 358-368, (1946)

[4] Astley R. J., and Cummings A. " A Finite Element Scheme for Attenuation in Ducts Lined with Porous Material: Comparision with Experiment", Journal of Sound and Vibration 116(4), 239-263, (1987)

[5] Munjal M. L., " Acoustics of Ducts and Mufflers", John Wiley, New York, (1987)

[6] Bolton J. S., Shiau N. M., and Kang, Y.J., " Sound Transmission through Multi-Panel Structures Lined with Elastic Porous Material", Journal of Sound and Vibration 191(2), 317-347, (1996)

[7] Zwikker C. and Kosten C. W., " Sound Absorbing Materials", New York: Elsevier, (1949)

[8] Morse P. M., and Ingard, K. U., " Theoretical Acoustics", New York: McGraw-Hill, (1968)

[9] Craggs A., " A Finite Element Model for Acoustically Lined Small Rooms", Journal of Sound and Vibration 108(2), 327-337, (1986)

[10] Hull A. J., " An Eigenvalue Based Acoustic Impedance Measurement Technique", Journal of Vibrations and Acoustics 61(1), 498-503, (1978)

[11] Craggs A., " Coupling of Finite Element Acoustic Absorption Models", Journal of Sound and Vibration 66(4), 605-613, (1979)